PHYSICAL REVIEW B **88**, 161305(R) (2013)

Observation of the intrinsic spin Hall effect in a two-dimensional electron gas

F. G. G. Hernandez,[1,*] L. M. Nunes,[1] G. M. Gusev,[1] and A. K. Bakarov[2]
[1]*Instituto de Física, Universidade de São Paulo, Caixa Postal 66318, CEP 05315-970, São Paulo, SP, Brazil*
[2]*Institute of Semiconductor Physics, Novosibirsk 630090, Russia*

(Received 7 June 2013; revised manuscript received 10 September 2013; published 29 October 2013)

The experimental demonstration of the spin Hall effect in a high mobility two-dimensional electron system is reported. The spatial dependence is studied by Kerr rotation as a function of the external magnetic field using an applied electric field amplitude and direction as control parameters. We observe that the effect is robust in a bilayer structure with a nonzero Rashba coefficient displayed by an electrically controllable internal magnetic field, a large spin Hall conductivity in the range of the universal intrinsic value, and a mobility-enhanced spin diffusion constant. With the application of an unidirectional electric field, the role of the spin drift was also studied. The data was analyzed following both phenomenological and microscopic approaches and compared with experimental references in a single-layer configuration.

DOI: 10.1103/PhysRevB.88.161305 PACS number(s): 72.25.Dc, 71.70.Ej, 73.21.Fg, 85.75.−d

A relativistic phenomenon has become of major relevance in the quest for spintronic devices: the spin-orbit interaction (SOI).[1] It opens a path for promising applications in semiconductor heterostructures such as spin field-effect transistors,[2] due to the SOI arising from the bulk and structural inversion asymmetry (Dresselhaus and Rashba SOI).[3,4] Large advances[5] have been made in recent years in the generation of current-induced spin polarization[6,7] in addition with the observation of the spin Hall effect (SHE) in *n*-type epilayers.[8–12] Renewed interest in the study of SOIs in two-dimensional (2D) systems is driven by the tuning possibility of the Rashba coefficient α by an external voltage, avoiding the need for magnetic fields for spin manipulation.[13–20] However, experimental observations of the SHE in such structures are still very limited, and only two groups have reported on the intrinsic SHE for holes[21] and the extrinsic SHE for electrons,[22] A great deal of debate still remains about the existence of an intrinsic SHE in 2D electron gases where the dc spin Hall conductivity due to intrinsic mechanisms was predicted to vanish when considering the extrinsic contribution by a small concentration of impurities.[23–25]

In the search for a system where the SHE may be robust, the multilayer configuration appears to have exceptional features.[26–28] For two-subband systems without coupling, the SHE has been recently predicted due to an intersubband-induced spin-orbit interaction which has the functional form of a Rashba term.[29–31] Even for symmetrically doped quantum wells, where the Rashba SOI contribution was demonstrated to vanish in single-layer systems,[32] this new SOI gives a nonzero ballistic spin Hall conductivity.[29] For a bilayer, assembled by the coupling of the two subbands using tunneling as an additional control parameter, a magnified spin Hall conductivity has been calculated that is nonzero even in the presence of impurities,[33] contrary to the single-layer case.

Here, we address the study of the SHE in a two-dimensional electron gas (2DEG) in a clean limit. We explore the robustness of the effect for a bilayer configuration and compare it to a single-layer sample that has been identically grown. We found spatially resolved out-of-plane spin accumulation with a Hanle curve dependence on the external (B_{ext}) and internal (B_{in}) magnetic fields, and with amplitude given by spin Hall conductivity (σ^{SH}) in the range of the intrinsic universal value. The control of accumulation peaks by the electric field (E) direction and the spin drift role were also demonstrated. Furthermore, signals near the voltage leads may indicate the existence of intrinsic spin Hall currents. The observation of these remarkable characteristics, together with the absence of a SHE signal in the single-layer sample, suggests that an intrinsic mechanism should be responsible for the measured SHE.

Figure 1(a) shows the calculated potential for a 45 nm wide GaAs quantum well with the associated symmetric (S) and antisymmetric (AS) wave functions for the two lowest subbands. Due to the Coulomb repulsion of the electrons in the wide quantum well that is doped in both barriers, the charge distribution results in a bilayer electron system with a soft barrier inside the well. For such wide wells, the Dresselhaus SOI was measured to be low as the variation in the size quantization of the wave vector z component modifies the linear coefficient β_1.[34,35] Electrical transport measurements determine a high electron density $n_s = 9.2 \times 10^{11}$ cm^{-2}, a mobility of $\mu = 1.9 \times 10^6$ cm^2/V s, and a subband separation of $\Delta_{\text{SAS}} = 1.4$ meV.[36] The signature of the SHE is also shown in Fig. 1(a), where opposite spins accumulate near the edges of the Hall bar when a small E is applied. An offset that is linear in B_{ext} has been subtracted from each scan. We labeled the center of the channel as $x = 0$, and $x = \pm 100$ μm are the Hall bar edges. Figure 1(c) shows the device geometry and the experimental configuration with E applied perpendicular to B_{ext}. A second sample containing a narrow 14 nm single quantum well with the same mobility and electron concentration in an identically layered heterostructure was also measured and the SHE signal was not observed [see Fig. 1(b)]. Thus, we confirm that any existing SHE mechanism in our samples can survive only in the bilayer configuration and it does not depend on the impurity level. Later we will add this result to the large σ^{SH} to relate our findings to an intrinsic mechanism.

Note that the high mobility is another relevant figure in this present Rapid Communication, which is more than three orders of magnitude larger than a previous study of the extrinsic SHE in a 2DEG.[22] For the application of E, we must consider that

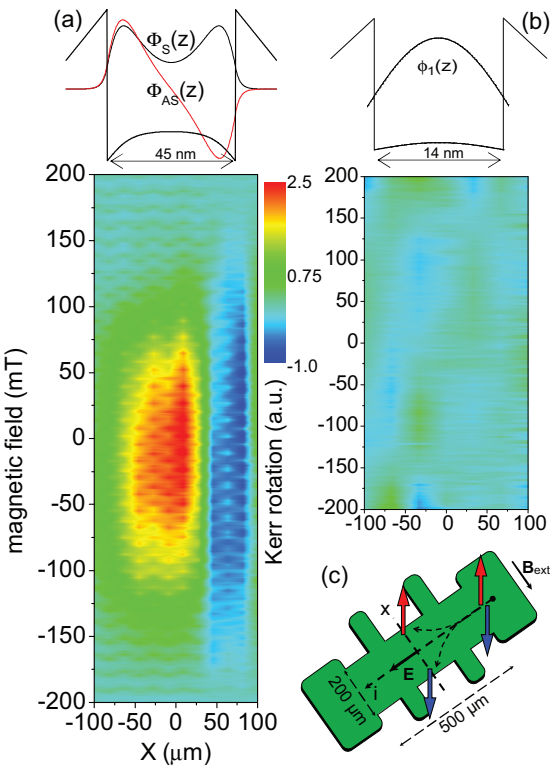

FIG. 1. (Color online) One-dimensional spatial profile of the spin accumulation as a function of B_{ext} at $E = 0.6\,\mathrm{mV}/\mu\mathrm{m}$ for (a) bilayer and (b) single-layer samples with the calculated well potential and the associated wave functions. (c) Device configuration sketching the spatial separation of opposite spins.

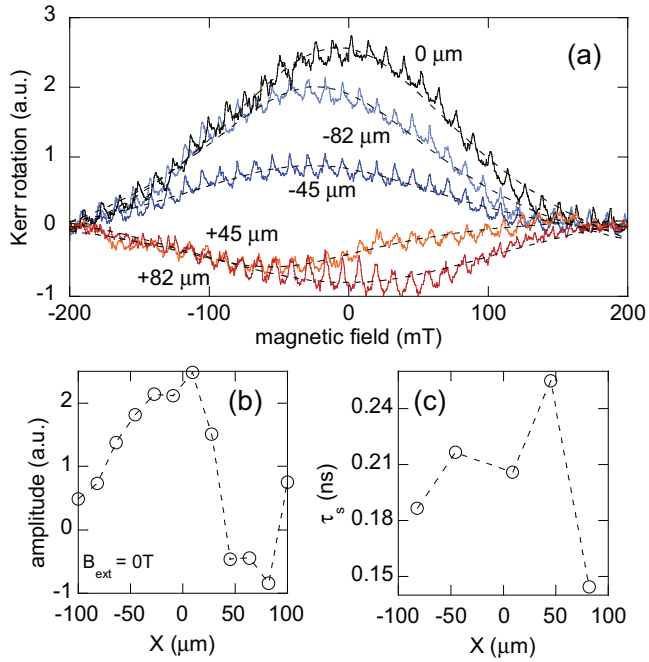

FIG. 2. (Color online) (a) B_{ext} scans of the KR signal at different probe positions. The dashed lines show the Hanle curve fits. (b) Spatial dependence of the KR amplitude at $B_{ext} = 0$. (c) Spin lifetime fitted in (a). Probe power: 150 μW, and $V_{rms} = 2.5$ V.

high μ results in a low channel resistance ($R_C = 10\ \Omega$) so that the voltage drops mainly at the contacts, reducing considerably the effective E inside the channel ($E = V_C/l$). The fabrication of quality ohmic contacts produced a total device resistance $R_T = 110\ \Omega$ from where the voltage drop in the channel is 9% of that supplied. A sine wave with an adjustable maximum peak amplitude $\pm E$ and a fixed frequency of 1.1402 kHz was used for lock-in detection. In the present analysis, the amplitude of the applied voltage will be labeled by the root mean square value (V_{rms}) so it can be directly compared with previous reports using square waves.

The 2DEG spin polarization was optically probed using Kerr rotation (KR) as it is a recognized powerful tool for SHE mapping[8] and the characterization of spin-orbit interactions in 2DEG.[37–39] A mode-locked Ti:sapphire laser was used, emitting pulses with 100 fs duration at a rate (f_{rep}) of 76 MHz. The laser was linearly polarized and tuned to the absorption edge of the quantum well (QW) samples. The sample was immersed in a variable temperature insert of a superconductor magnet in Voigt geometry. The probe laser was focused to $\sim$20 μm spot using a lens outside the magnet. The probe beam polarization was not modulated and its rotation was detected by coupled photodiodes. The spin accumulation was tested using two different levels of probe power (150 μW and 2.5 mW). The temperature was kept constant at $T = 5$ K.

Line cuts in Fig. 1(a) as function of B_{ext} are plotted in Fig. 2(a) for positions along the bar width. Note that a fast oscillation with field period $\Delta B_{ext} = 12.5$ mT is superimposed in the SHE peaks. This signal was not detected in the single-layer sample and displays a behavior similar to resonant spin amplification (RSA) using the pump-probe technique at a fixed time delay.[40] Nevertheless, there is no extra pump laser and the detection is locked to the voltage frequency here. In a complementary experiment using time-resolved KR (TRKR),[41] we observed that long-lived spin oscillations with a dephasing time T_2^* similar to $1/f_{rep}$ can be initiated with a linearly polarized pump in the bilayer sample. Briefly, we assume that the probe laser is acting also as an optical pump on the in-plane, current-induced spin polarization. Such optical pumping takes that spin polarization to the out-of-plane direction and leads to precession around the transverse B_{ext} in a RSA-like signal. For clarity, we will focus on the spin accumulation related to the SHE as we conclude that both effects have an independent origin. Although a previous study showed that a linearly polarized laser could generate electron spin coherence,[42] such optical amplification of electrically induced spin polarization requires further investigation, and an extended, detailed report will be published elsewhere.[43]

The data in Fig. 2(a) can be modeled as the depolarization of out-of-plane spin accumulation following a Hanle effect curve.[22] The line shape of the Hanle effect curve is strongly related to the direction of the precessing spins being symmetric (out-of-plane polarization) or antisymmetric (in-plane polarization).[44,45] In the $B_{ext} \perp E$ configuration, the in-plane, current-induced spin polarization cannot precess around the total B (B_T) and it is not detected by polar KR so the curve is expected to be symmetric.[7] The curves can be fitted by a Lorentzian form $A/[(\omega_L \tau_s)^2 + 1]$ with half-width $B_{1/2} =$

$\hbar/(g\mu_B\tau_s)$, where A is the KR amplitude, $\omega_L = g\mu_B B_{\rm ext}/\hbar$ is the Larmor frequency with the electron g factor g, Bohr magneton μ_B, Planck's constant $\hbar$, and τ_s is the spin lifetime. A g-factor magnitude of $|g| = 0.44$ was measured by TRKR for the wide GaAs well. In Fig. 2(a), the peak center shifts toward negative $B_{\rm ext}$ for some probe positions, revealing a spatially dependent $B_{\rm in} \parallel B_{\rm ext}$ arising from the SOI. Figures 2(b) and 2(c) show the results for the amplitude at $B_{\rm ext} = 0$ and τ_s at the positions plotted in Fig. 2(a). The spin polarization peaks present a spatially asymmetric broad structure at zero field with a peak-to-peak separation of about 80 μm. The spatial asymmetry in the amplitude of the two opposite spin polarization peaks was previously observed in GaAs layers and 2DEG as well as the spatial dependence of τ_s.[8,10,22] The short spin lifetime is expected in the Fermi liquid regime for a high density 2DEG.[46] At the center of the Hall bar, the largest positive signal is obtained but with a shorter τ_s compared to the edge peaks, and it could be related to the spin drift resulting from the symmetric E utilized for lock-in detection,[10] as we will discuss below. Using a drift-diffusion model, the spin diffusion constant (D) can be obtained from the relation for the spin diffusion length $L_s = \sqrt{D\tau_s}$. From the spatial scan in Fig. 2(b), $L_s = 25$ μm, which is similar to the charge mean free path for this sample. Setting $\tau_s = 0.25$ ns, the data gives $D = 2.5$ m^2/s, consistent with a mobility increase of 10^3 if compared to Refs. 9 and 22.

Considering the dense 2DEG in our system, the probe power influence was tested by raising the level from 150 μW to 2.5 mW. Figure 3(a) shows the SHE in such a condition where the peak-to-peak spatial separation remained constant compared to Fig. 1, but the $B_{\rm ext}$ scans present a more asymmetric Hanle curve. The curve asymmetry is reflected by the opposite spin polarizations at different $B_{\rm ext}$ in the same sample position next to the left side. At the right edge, a positive signal was measured which could be a manifestation of the predicted intrinsic spin Hall currents near the side voltage leads.[47] The RSA oscillations appeared to be stronger over the whole sample since they are amplified by the high probe power and broader due to a reduction of the dephasing time, also expected under high optical pumping. Together with the line-shape change, the linewidth is narrower, as displayed in Fig. 3(b). As discussed above, such asymmetry in $B_{\rm ext}$ could be related to an in-plane spin polarization that is possibly optically generated as the line-shape modification was observed only under high probe power. As the symmetric component still dominates for large voltages [see Fig. 3(c)], we will not modify the Hanle model for the electrically induced spin polarization by adding an asymmetric, optically generated component. Figure 3(c) displays the SHE dependence on the magnitude of E where A, $B_{1/2}$, and $B_{\rm in}$ were fitted [see results in Fig. 4(a)]. Obtained from the Lorentzian peak shift ($B_T = B_{\rm in} + B_{\rm ext} = 0$ at the peak), $B_{\rm in}$ changes sign and increases linearly with E with a slope (188 ± 14) mT/(mV/μm), and then decreases with a slightly smaller slope. Also, the data show a fast increase in the accumulation amplitude with a slope 0.72 ± 0.04, followed by a sharp decrease for higher E, possibly due to heating. $B_{\rm in}$ and A have maximum values at the same E. The peak width does not display a clear trend for increasing E. Also we note that there is a threshold for the SHE observation around 1.75–2 V ($\sim$0.5 mV/μm).

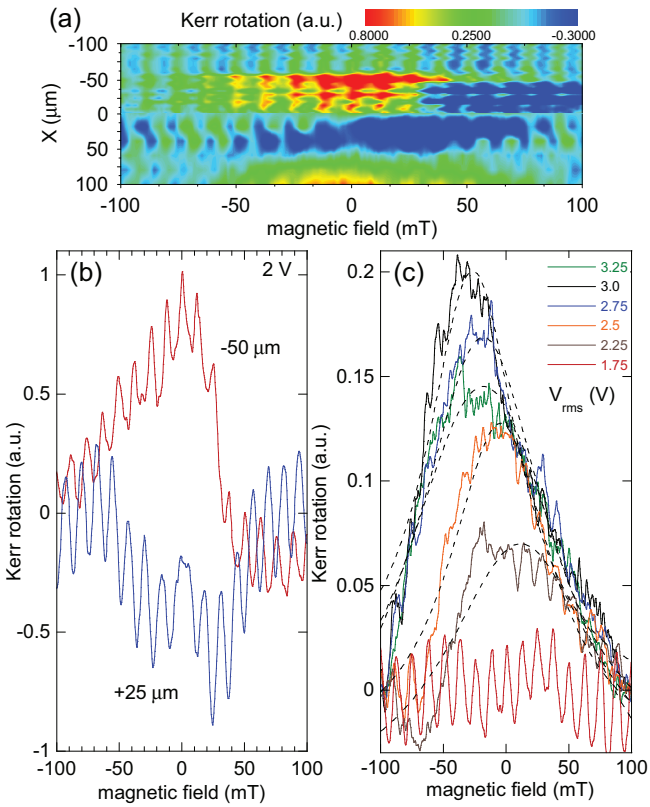

FIG. 3. (Color online) (a) One-dimensional spatial profile as a function of $B_{\rm ext}$ measured with 2.5 mW probe power. (b) Line cuts in (a) for the polarization peak positions. (c) Positive peak dependence on the applied voltage. The dashed lines show the Hanle curve fits.

Figure 4(b) demonstrates the polarization inversion of the SHE peaks by reversing the function of the source-drain contacts. The side voltage probes can also be used as the current source and drain for the case with $B_{\rm ext} \parallel E$ and show no spin accumulation. Finally, we note that the electric field changes its direction during the time cycle of V_C so that there could be an effect on the spin drift due to symmetric current flow.[10] We added a negative dc voltage offset to produce a unidirectional electric field oscillating in amplitude between zero and $-E$. Figure 4(c) shows the result, with low probe power, for $V_{\rm dc} = -V_p = -2.5$ V, where both accumulation peaks are clearly displayed in opposite sides, compared to Fig. 1(a). Furthermore, the signal at the center of the Hall bar vanishes and L_s is promoted, revealing the main role of the spin drift in the SHE. Again, a signal is detected next to the lateral voltage leads at $x = \pm 100$ μm, as commented above.

The experimental spin accumulation can be traced to the SHE phenomenological treatment[48] by the spin density at the edges: $A \propto n_0 = \beta n_s E L_s/D$, where $\beta = \gamma\mu$ and γ is a parameter that accounts for the SOI strength. The positive peak in Fig. 1(a), for example, has an amplitude of 30 μrad that should encompass about $N = 100$ electron spins under the probe spot area.[8,12] Fixing an approximate number of ten spins for the minimum signal detection, we estimate a range of $N = 10$–100 electron spins. It sets a low limit to $n_0 = 3.18 \times 10^6$ cm^{-2} and a degree of polarization

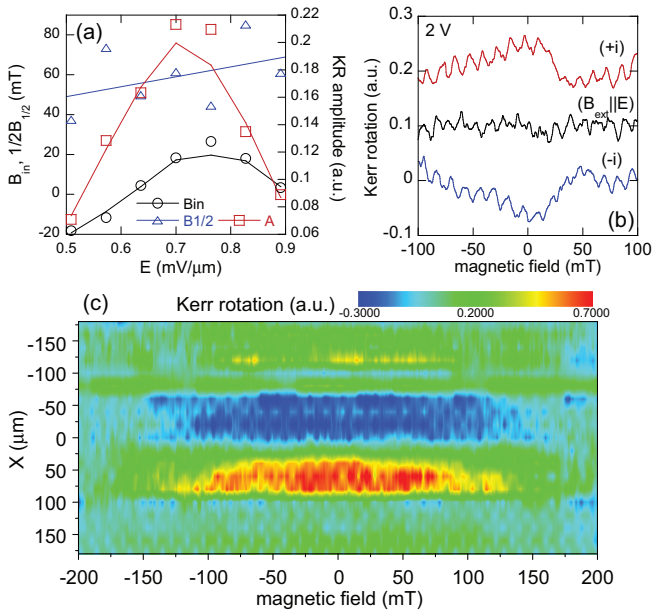

FIG. 4. (Color online) (a) Dependence of $B_{\rm in}$, $B_{1/2}$, and KR amplitude on E. The lines are a guide to the eyes and the data point size represents the error bar. (b) Inversion of the positive polarization peak by switching the source-drain contacts. The labels indicate the geometry compared to Fig. 1 ($+i$). (c) One-dimensional SHE spatial profile as a function of $B_{\rm ext}$ with unidirectional E.

$n_0/n_s = 3.45 \times 10^{-6}$. The product $EL_s/D = 0.006$ V s/m^2 defines $\beta = 5.76 \times 10^{-4}$ m^2/V s and $\gamma = 2.88 \times 10^{-6}$. Remarkably, we note that the high mobility factor inside β compensates the low E, allowing the accumulation of an optically measurable spin polarization.

Furthermore, we can evaluate the spin Hall conductivity $\sigma^{\rm SH} = j_s/E$, where j_s is the spin current density (in units of charge current) resulting from an applied E.[23] The density of the spin accumulation produced by the spin currents can be estimated by $n_0 = (\sigma^{\rm SH}/e)(EL_s/D)$ in the two-dimensional system.[8] Using the above range for N, the data gives $\sigma^{\rm SH} = 0.1\text{–}1\sigma_0^{\rm SH}$, where $\sigma_0^{\rm SH} = e^2/(8\pi\hbar) \simeq (100\ {\rm k}\Omega)^{-1}$ is the 2D universal intrinsic spin Hall conductivity calculated in the clean limit.[49] Thus, the data indicates that a low spin Hall resistivity $\rho^{\rm SH} = 1/\sigma^{\rm SH} = 0.1\text{–}1$ MΩ in the bilayer system is responsible for the observation of the SHE. The result agrees with the theoretical prediction of a robust SHE in the presence of impurities for a bilayer electron system with $\sigma^{\rm SH}$ close to $\sigma_0^{\rm SH}$ when $\mu \simeq 10^6$ cm^2/V s.[33] Together with the phenomenological expression, we obtain $\beta n_s = \sigma^{\rm SH}/e$, which verifies that the estimated spin accumulation density range holds to the $\sigma_0^{\rm SH}$ limit. Scaling $\sigma^{\rm SH}$ to a bulk sample by $\sigma_{\rm 3D}^{\rm SH} \simeq \sigma^{\rm SH} k_F$, where k_F is the Fermi wave vector,[50] the sample resistivity will be $\rho_{\rm 3D}^{\rm SH} = 1\text{–}10$ kΩ μm. This value gives a conductivity increase of 10^3 for the ratio between the present case and previous bulk reports of the extrinsic SHE and also agrees with the βn_s ratio.

In conclusion, we experimentally observed the spin Hall effect for a clean 2DEG confined in a bilayer structure. Two opposite spin accumulation peaks were detected near the Hall bar edges at zero external magnetic field under an applied electric field where the spin drift played a major role. The peaks line shape in B appeared to depend on the probe power level and revealed a short spin lifetime on the order of 0.5 ns. The spin diffusion constant was estimated to be mobility enhanced, of approximately 2.5 m^2/s, for a diffusion length of 25 μm. An electrically tunable internal magnetic field was measured, indicating a nonzero Rashba coefficient. The absence of SHE signal in the single-layer sample with the same impurity level and electron concentration, together with a large spin Hall conductivity in the range of $\sigma_0^{\rm SH}$, supports the association of the experimental findings to a robust intrinsic mechanism. This study reinforces the interest of investigations on the SHE and spin helix formation in multilayer systems and opens a path for the study of these effects in the clean limit.

Financial support of this work by Grants No. 2009/15007-5, No. 2010/09880-5, and No. 2013/03450-7, São Paulo Research Foundation (FAPESP), and CNPq is acknowledged. All measurements were done in the LNMS at DFMT-IFUSP.

*Corresponding author: felixggh@if.usp.br

[1] H. Feshbach and F. Villars, Rev. Mod. Phys. **30**, 24 (1958); J. D. Bjorken and S. D. Drell, *Relativistic Quantum Mechanics* (McGraw-Hill, New York, 1965).

[2] S. Datta and B. Das, Appl. Phys. Lett. **56**, 665 (1990); J. C. Egues, G. Burkard, and D. Loss, *ibid.* **82**, 2658 (2003).

[3] G. Dresselhaus, Phys. Rev. **100**, 580 (1955).

[4] E. I. Rashba, Sov. Phys. Solid State **2**, 1109 (1960); Y. A. Bychkov and E. I. Rashba, J. Phys. C **17**, 6039 (1984); JETP Lett. **39**, 78 (1984).

[5] For a review, see *Semiconductor Spintronics and Quantum Computation*, edited by D. D. Awschalom, D. Loss, and N. Samarth (Springer, Berlin, 2002); I. Zutic, J. Fabian, and S. Das Sarma, Rev. Mod. Phys. **76**, 323 (2004).

[6] Y. K. Kato, R. C. Myers, A. C. Gossard, and D. D. Awschalom, Phys. Rev. Lett. **93**, 176601 (2004).

[7] N. P. Stern, S. Ghosh, G. Xiang, M. Zhu, N. Samarth, and D. D. Awschalom, Phys. Rev. Lett. **97**, 126603 (2006).

[8] Y. K. Kato, R. C. Myers, A. C. Gossard, and D. D. Awschalom, Science **306**, 1910 (2004).

[9] V. Sih, W. H. Lau, R. C. Myers, V. R. Horowitz, A. C. Gossard, and D. D. Awschalom, Phys. Rev. Lett. **97**, 096605 (2006).

[10] N. P. Stern, D. W. Steuerman, S. Mack, A. C. Gossard, and D. D. Awschalom, Appl. Phys. Lett. **91**, 062109 (2007).

[11] N. P. Stern, D. W. Steuerman, S. Mack, A. C. Gossard, and D. D. Awschalom, Nat. Phys. **4**, 843 (2008).

[12] S. Matsuzaka, Y. Ohno, and H. Ohno, Phys. Rev. B **80**, 241305(R) (2009).

[13] A. Khaetskii, Phys. Rev. B **73**, 115323 (2006).
[14] A. V. Shytov, E. G. Mishchenko, H.-A. Engel, and B. I. Halperin, Phys. Rev. B **73**, 075316 (2006).
[15] R. Raimondi, P. Schwab, C. Gorini, and G. Vignale, Ann. Phys. **524**, 153 (2012).
[16] O. E. Raichev, Phys. Rev. B **75**, 205340 (2007); Int. J. Mod. Phys. B **23**, 2566 (2009).
[17] C. Wang, H. T. Cui, and Q. Lin, Phys. Status Solidi B **246**, 2301 (2009).
[18] E. I. Rashba and Al. L. Efros, Phys. Rev. Lett. **91**, 126405 (2003); Appl. Phys. Lett. **83**, 5295 (2003).
[19] H.-A. Engel, E. I. Rashba, and B. I. Halperin, Phys. Rev. Lett. **98**, 036602 (2007).
[20] Z. Wilamowski, W. Ungier, and W. Jantsch, Phys. Rev. B **78**, 174423 (2008).
[21] J. Wunderlich, B. Kaestner, J. Sinova, and T. Jungwirth, Phys. Rev. Lett. **94**, 047204 (2005).
[22] V. Sih, R. C. Myers, Y. K. Kato, W. H. Lau, A. C. Gossard, and D. D. Awschalom, Nat. Phys. **1**, 31 (2005).
[23] H.-A. Engel, E. I. Rashba, and B. I. Halperin, *Handbook of Magnetism and Advanced Magnetic Materials* (Wiley, Chichester, 2007).
[24] J. I. Inoue, G. E. W. Bauer, and L. W. Molenkamp, Phys. Rev. B **70**, 041303 (2004).
[25] W. Yang, K. Chang, and S.-C. Zhang, Phys. Rev. Lett. **100**, 056602 (2008).
[26] D. M. Gvozdić and U. Ekenberg, Appl. Phys. Lett. **90**, 053105 (2007).
[27] U. Ekenberg and D. M. Gvozdić, Phys. Rev. B **78**, 205317 (2008).
[28] M. Akabori, S. Hidaka, H. Iwase, S. Yamada, and U. Ekenberg, J. Appl. Phys. **112**, 113711 (2012).
[29] E. Bernardes, J. Schliemann, M. Lee, J. C. Egues, and D. Loss, Phys. Rev. Lett. **99**, 076603 (2007).
[30] R. S. Calsaverini, E. Bernardes, J. C. Egues, and D. Loss, Phys. Rev. B **78**, 155313 (2008).
[31] M. Lee, M. O. Hachiya, E. Bernardes, J. C. Egues, and D. Loss, Phys. Rev. B **80**, 155314 (2009).
[32] V. Lechner, L. E. Golub, P. Olbrich, S. Stachel, D. Schuh, W. Wegscheider, V. V. Bel'kov, and S. D. Ganichev, Appl. Phys. Lett. **94**, 242109 (2009).
[33] P.-Q. Jin and Y.-Q. Li, Phys. Rev. B **76**, 235311 (2007).
[34] M. Studer, M. P. Walser, S. Baer, H. Rusterholz, S. Schön, D. Schuh, W. Wegscheider, K. Ensslin, and G. Salis, Phys. Rev. B **82**, 235320 (2010).
[35] M. P. Walser, U. Siegenthaler, V. Lechner, D. Schuh, S. D. Ganichev, W. Wegscheider, and G. Salis, Phys. Rev. B **86**, 195309 (2012).
[36] S. Wiedmann, G. M. Gusev, O. E. Raichev, A. K. Bakarov, and J. C. Portal, Phys. Rev. B **84**, 165303 (2011).
[37] L. Meier, G. Salis, I. Shorubalko, E. Gini, S. Schön, and K. Ensslin, Nat. Phys. **3**, 650 (2007).
[38] M. Studer, S. Schön, K. Ensslin, and G. Salis, Phys. Rev. B **79**, 045302 (2009).
[39] L. Meier, G. Salis, E. Gini, I. Shorubalko, and K. Ensslin, Phys. Rev. B **77**, 035305 (2008).
[40] J. M. Kikkawa and D. D. Awschalom, Nature (London) **397**, 139 (1999).
[41] See Supplemental Material at http://link.aps.org/supplemental/10.1103/PhysRevB.88.161305 for details on the resonant spin amplification data.
[42] K. Schmalbuch, S. Göbbels, Ph. Schäfers, Ch. Rodenbücher, P. Schlammes, Th. Schäpers, M. Lepsa, G. Güntherodt, and B. Beschoten, Phys. Rev. Lett. **105**, 246603 (2010).
[43] F. G. G. Hernandez *et al*. (unpublished).
[44] S. Kuhlen, K. Schmalbuch, M. Hagedorn, P. Schlammes, M. Patt, M. Lepsa, G. Güntherodt, and B. Beschoten, Phys. Rev. Lett. **109**, 146603 (2012).
[45] S. A. Crooker, M. Furis, X. Lou, P. A. Crowell, D. L. Smith, C. Adelmann, and C. J. Palmstrøm, J. Appl. Phys. **101**, 081716 (2007).
[46] R. I. Dzhioev, K. V. Kavokin, V. L. Korenev, M. V. Lazarev, B. Ya. Meltser, M. N. Stepanova, B. P. Zakharchenya, D. Gammon, and D. S. Katzer, Phys. Rev. B **66**, 245204 (2002).
[47] I. Adagideli and G. E. W. Bauer, Phys. Rev. Lett. **95**, 256602 (2005).
[48] M. I. Dyakonov and V. I. Perel, Pis'ma Zh. Eksp. Teo. Fiz. **13**, 657 (1971) [Sov. Phys. JETP Lett. **13**, 467 (1971)]; M. I. Dyakonov, Phys. Rev. Lett. **99**, 126601 (2007); Int. J. Mod. Phys. B **23**, 2556 (2009).
[49] J. Sinova, D. Culcer, Q. Niu, N. A. Sinitsyn, T. Jungwirth, and A. H. MacDonald, Phys. Rev. Lett. **92**, 126603 (2004).
[50] B. A. Bernevig and S.-C. Zhang, Phys. Rev. B **72**, 115204 (2005).